

TISSUE ENGINEERING: Part A

Volume 00, Number 00, 2025

^a Mary Ann Liebert (NY), LLC

DOI: <https://doi.org/10.1177/19373341251404075>

ORIGINAL ARTICLE

Tissue-Inducing Biomaterials for Cardiac Tissue Regeneration and Repair

Muhammad Shafiq, PhD,^{1,*} Qasim A. Majid, PhD,^{2,3,*} Muhammad Rafique, PhD,⁴
and Virpi Talman, BSc, MSc, PhD^{1,2}

Abstract

Ischemic cardiac injury, arising due to myocardial infarction (MI), ischemia-reperfusion injury (IRI), and other ischemia-associated forms of cardiac damage, remains a major clinical challenge. The irreversible loss of cardiomyocytes (CM) from within the myocardium, together with oxidative stress, and inflammation, creates a complex post-MI milieu that is not readily addressed by existing therapeutic strategies. Cardiac tissue engineering (CTE) solutions that combine advanced biomaterials with either stem cell-derived cardiovascular cells, their derivatives (such as extracellular vesicles and exosomes), or other bioactive compounds (including chemokines and cytokines) are being developed to repair and regenerate the infarcted human heart. This review highlights the state-of-the-art strategies that utilise cutting-edge technologies to develop tissue-inducing biomaterial solutions for cardiac regeneration and repair, with particular emphasis on (i) integrating biomaterials with cells in strategies undergoing clinical investigation, (ii) incorporating cellular derivatives into biomaterial scaffolds, and (iii) designing and evaluating intrinsically functional biomaterials. This review aims to provide both a theoretical foundation and future perspectives for the innovation and optimisation of next generation tissue-inducing biomaterial-based strategies for cardiac tissue regeneration and repair.

Keywords: myocardial infarction, cardiac patch, in situ tissue repair, cardiovascular tissue repair, human-induced pluripotent stem cell-derived cardiomyocytes, exosomes

Impact statement: Ischemic heart disease is the leading cause of death and accounts for approximately one third of all deaths in developed countries, with more than 64 million people currently living with heart failure. Alongside substantial loss of cardiomyocytes (CMs),

myocardial infarction (MI) leads to adverse cardiac remodelling, progressive weakening of the cardiac muscle, and scar tissue formation (fibrosis). Authors review cutting-edge technological advancements in biomaterials with intrinsic ability to induce endogenous tissue repair, with particular emphasis on intrinsically functional biomaterials and the integration of these biomaterials with cells and/or cytokines or chemokines to enhance therapeutic efficacy.

Affiliations

¹ Research Centre for Integrative Physiology & Pharmacology, Institute of Biomedicine, Faculty of Medicine, University of Turku, Turku, Finland.

² Drug Research Program and Division of Pharmacology and Pharmacotherapy, Faculty of Pharmacy, University of Helsinki, Helsinki, Finland.

³ Department of Pharmacology and Toxicology, Institute of Pharmaceutical Sciences, University of Graz, Graz, Austria.

⁴ School of Biomedical Engineering and Med-X Research Institute, Shanghai Jiao Tong University, Shanghai, 200240, China.

*Both authors contributed equally and are cofirst authors

***Corresponding Author:**

Virpi Talman
Faculty of Medicine, Institute of Biomedicine
University of Turku
Kiinamylynkatu 10
FI-20520 Turku
Finland

Email: virpi.talman@utu.fi

Tel. +358 50 590 6676

Received: August 6, 2025

Accepted: October 25, 2025

Online Publication Date: December 19, 2025

Introduction

Heart failure with reduced ejection fraction (HFrEF), defined by left ventricular ejection fraction below 40%, accounts for over 50% of heart failure cases and is often caused by myocardial infarction (MI)^{1,2} which can lead to the loss of one billion cardiomyocytes (CMs) in the left ventricle (LV). Whilst clinical advancements have improved immediate post-MI survival, the adult human heart cannot regenerate the damaged tissue due to the limited proliferation capacity of cardiomyocytes^{3,4} The contractile muscle tissue of the human adult LV is therefore replaced with a fibrotic scar that stabilises the heart but impairs contractility (Fig.1A)⁵ Whilst some species retain regenerative capacity throughout their lifespan, the human heart compensates through CM hypertrophy, which eventually becomes pathological and leads to progressive cardiac dysfunction.

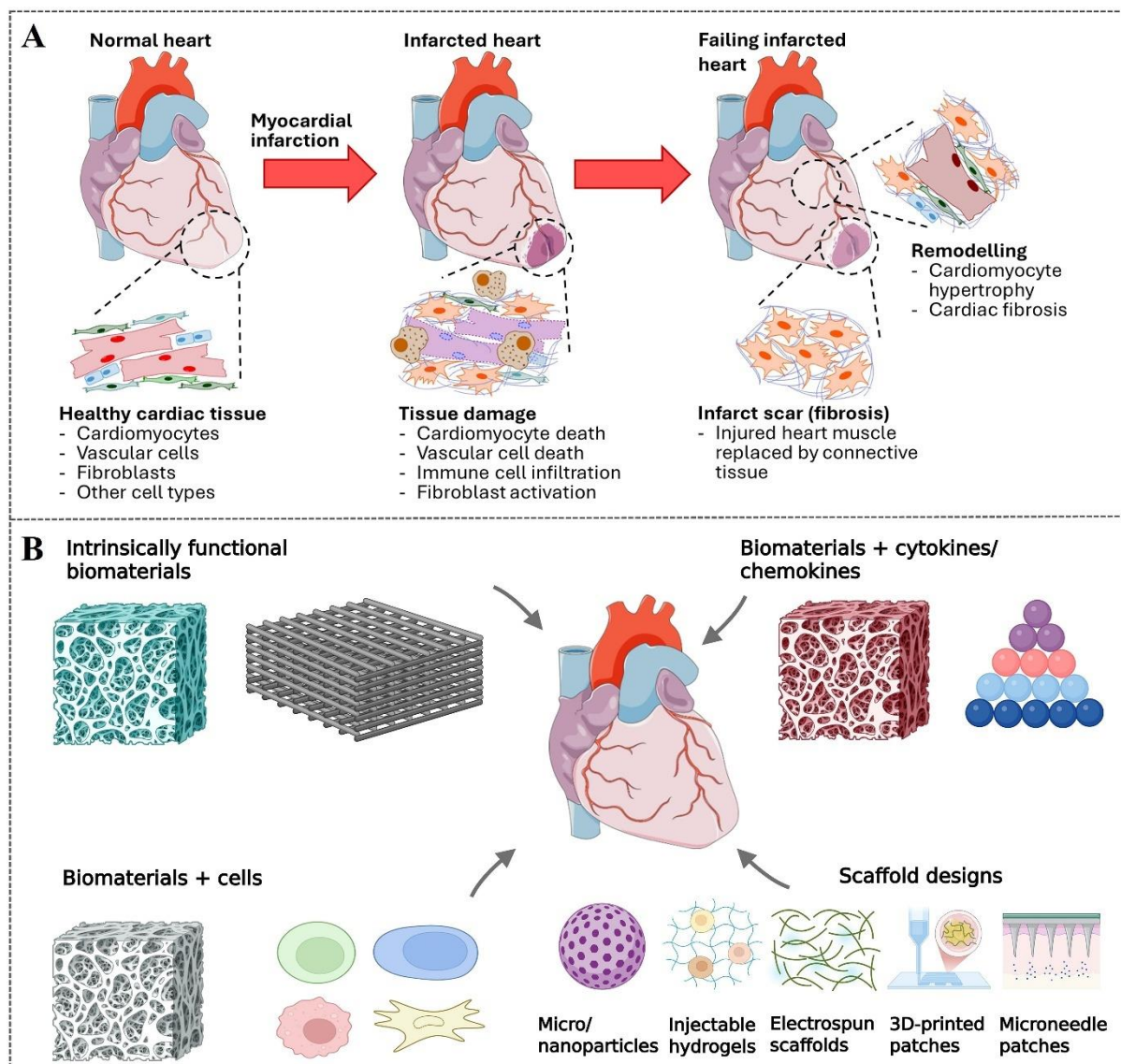


FIG. 1. Pathophysiological mechanisms of myocardial infarction (MI) and biomaterial-based strategies for in situ cardiac regeneration and repair. (A) Following MI, necrotic cardiomyocytes in the infarct zone promote the infiltration of immune cells and activation of resident fibroblasts, resulting in further damage to the myocardium. A remodeling phase ensues as characterized by the deposition of a thick fibrotic scar that perturbs contractility and cardiomyocyte hypertrophy that contributes to ventricular dilation. (B) Various biomaterial-based strategies have been designed to enhance post-MI cardiac regeneration and repair. Heart illustrations were provided by Servier Medical Art (<https://smart.servier.com>), licensed under CC BY 4.0 (<https://creativecommons.org/licenses/by/4.0/>). Figure 1B was created in Biorender (<https://BioRender.com/mobd7aa>).

Cardiac tissue engineering (CTE) aims to restore myocardial function by either delivering exogenous cardiovascular cells (cell-based CTE) or stimulating endogenous cardiac regeneration using biomaterials and bioactive factors (cell-free CTE), such as growth factors, cytokines and chemokines, and extracellular vesicles (Fig. 1B). This review highlights emerging biomaterial-based approaches for cardiac regeneration, including (1) human induced pluripotent stem cell-derived cardiomyocytes (hiPSC-CMs) and cellular derivatives, (2) functionalised biomaterials, and (3) biomaterials containing bioactive cues for CTE.

Biomaterials, whether synthetic (e.g. polycaprolactone, PCL) or natural (e.g. collagen)⁶, must be biocompatible, non-immunogenic, and mechanically resilient to withstand continuous beating. Further, they should support the fabrication of complex 3D scaffolds that mimic myocardial architecture⁷ or provide structural and topographical cues that drive the maturation and alignment of cells seeded onto.⁸ The success of cell-based CTE strategies relies on the interplay between the scaffold and cellular components. Indeed, the composition of cardiac cell types used, particularly the inclusion of non-CMs, such as endothelial cells (ECs) may have profound consequences on the efficacy of the CTE solution.⁹

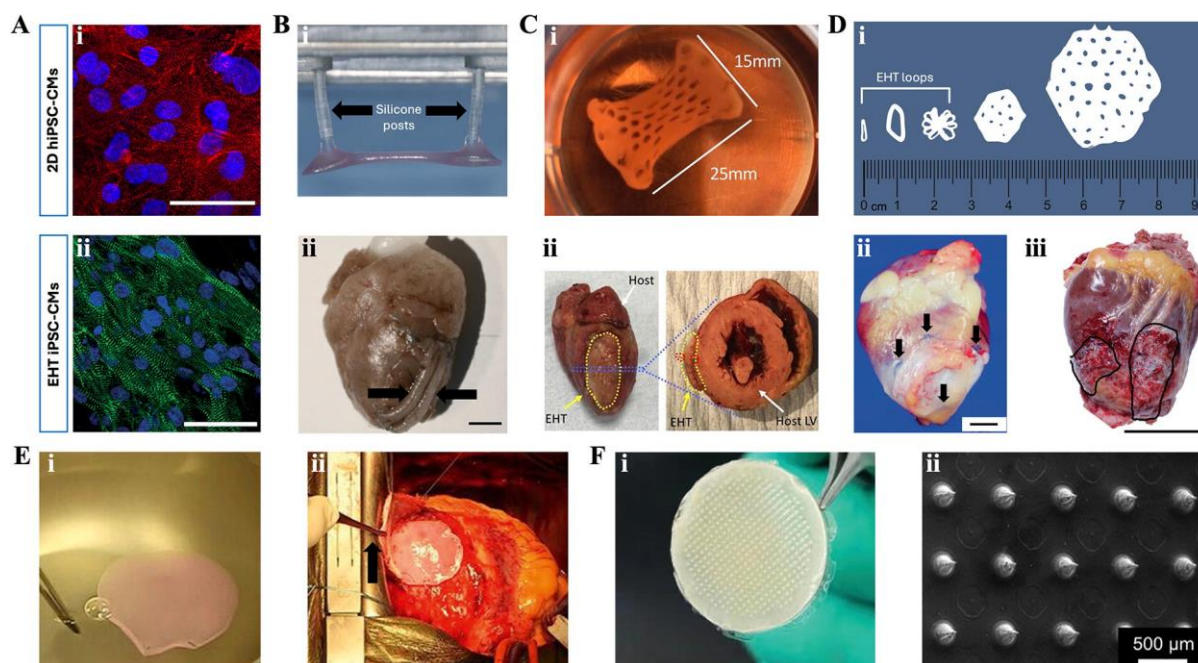


FIG. 2. CTE solutions that deliver exogenous cells or exosomes to the infarcted heart. (A) Immunofluorescent images of iPSC-CMs cultured in (i) 2D culture or (ii) within engineered heart tissues (EHTs). iPSC-CMs were stained for the cardiomyocyte marker α -actinin (red/green) and the nuclear marker Hoechst (blue). Scale bar represents 50 μ m. (B–F) Macroscopic images of (B) (i) EHT strips suspended between two silicone posts (highlighted by black arrows) and 2 EHT strips (black arrows) applied to the infarcted guinea pig heart. Scale bars represent 3 mm. (C) (i) Upscaled EHTs following 28 days of in vitro culture and (ii) following 2 weeks of application on the LV of healthy control rabbits. The EHT is delineated by the yellow line. (D) (i) Illustration of different EHT designs (from left to right): small EHT loops (1.5×10^6 cells/500 μ l), big EHT loops (2.5×10^6 cells/900 μ l), 5 big loops fused together, small EHT patch (10×10^6 cells/2 ml), and clinically-sized large EHT patch (40×10^6 cells/8 ml). Clinically-sized large EHT patches applied to (ii) rhesus macaque hearts for 6 months and (iii) to the infarcted human heart. (ii–iii) The black arrows highlight the sutures that adhere the EHT patch to the LV and the black circles delineate the EHT patches. Scale bars represent 10 mm and 5 cm, respectively. (E) hESC-derived SSEA-1+ cardiac progenitor-containing fibrin patches (i) prior to administration, (ii) placed onto the LV with the pericardial flap help by the tweezer (black arrow). (F) (i) Microneedle patch and (ii) scanning electron microscopy image of the microneedles within the patch. Scale bars represent 500 μ m respectively. Figures were adapted from: (Ai) Majid et al.,⁸; (Aii, Dii, iii) Jebran et al.,¹³; (B) Weinberger et al.,¹¹; (C) Jabbour and Owen et al.,¹²; (E) Menasché et al.,¹⁴; (F) Yuan et al.,¹⁵ and (Di) redrawn from Tiburcy et al.¹⁰ CM, cardiomyocyte; EHT, engineered heart tissue; hESC, human embryonic stem cell; LV, left ventricle; hiPSC-CM, human-induced pluripotent stem cell-derived cardiomyocytes.

CTE solutions that deliver exogenous cells

Engineered heart tissue/muscle (EHT/EHM, herein collectively referred to as a EHTs) are among the most advanced CTE solutions and are formed by encapsulating hiPSC-CMs within a fibrin or

collagen hydrogel suspended between flexible silicone posts (Fig. 2A, Fig. 2Bi, and Table 1). The spontaneous contractility of immature hiPSC-CMs in this setting induces uniaxial strain, promoting cellular alignment and maturation of hiPSC-CMs from a rounded, foetal-like morphology with poorly organised sarcomeres to an anisotropic, adult-like morphology with well-organised sarcomeres. (Fig. 2A).¹⁰⁻¹³

EHTs of different geometries, cell number, and cellular composition have been iteratively evaluated in pre-clinical models of HF_{rEF}, where they have been applied to the epicardial surface of the LV following MI or myocardial injury (Fig. 2B-D).¹⁴⁻¹⁷ Indeed, EHT strips comprised of 7 million hiPSC-derived cardiovascular cells (5×10^6 hiPSC-CMs and 2×10^6 hiPSC-ECs) were applied to the guinea pig heart (Fig. 2Bii) one-week post-cryoinjury and significantly improved fractional area change (FAC, the change in LV area between diastole and systole) despite relatively low (18%) retention of the administered hiPSC-cardiovascular cells, that remuscularised approximately.¹⁵ Upscaled EHTs containing 20×10^6 hiPSC-CMs similarly enhanced FAC in a rabbit model of MI, although minimal hiPSC-CM retention was reported one-month post-administration (Fig. 2C). Collagen-derived EHTs have also been upscaled to clinically relevant dimensions (4 cm^2) (Fig. 2Di)¹⁸ and evaluated in a rhesus macaque model of chronic HF (CHF).¹⁷ Five EHTs, each containing 40×10^6 rhesus macaque iPSC-CMs and -stromal cells were applied to the infarcted LV and significantly enhanced post-MI left ventricular ejection fraction (LVEF).

Table 1. Summary of the Cardiac Tissue Engineering Solutions That Deliver Exogenous Cells or Exosomes to the Infarcted Heart and Have Been Evaluated In Vivo.

| Biomaterial | Cells/ derivatives incorporated into patch | MI model/species | Follow-up | Outcome | Ref |
|---------------------------------------|---------------------------------------------------------------------------------------------------------------------------------------------------------|-----------------------------------------------------------------------------------------------------------------------|--------------------------------------------------------------------------|---------------------------------------------------------------------------------------------------------------------|-------------------------------------------------------------------------------------------------------------------------------------------------------------------------------------------------------------------------------------------------------------------------------------------------------------------------------------------------------------------------------------------------------------------------------------------------------------------------------------------------------------------------------------------|
| EHT loop Collagen type I | 2.5×10^6 hESC-CMs | Chronic MI model established 1 month post IRI at which point the patch was administered Male nude athymic rats | 28 days post-administration 110- and 220-days post-administration | Cardiac structure and function: Cardiac structure and function: Histology and retention: | 16 <ul style="list-style-type: none"> • LVEF was not enhanced following patch administration • Neither hESC-CM containing or irradiated EHTs improved ESV or EDV • Cell loss limited to first two weeks post-administration • $10 \pm 4\%$ average long term cell retention • Infiltration of host vasculature into the EHT • Few ($0.95 \pm 0.15\%$) proliferating hESC-CMs within EHT |
| EHT strips Bovine Fibrin (ogen) | EHT: 5.0×10^6 hiPSC-CMs with 2.0×10^6 hiPSC-ECs (or initially, HUVECs) EC patch: 7.0×10^6 hiPSC-ECs. | Cryoinjury of the LV with 2 of the same EHTs administered 7 days post injury. Female guinea pigs | 28 days post-administration 28 days post-administration | Cardiac structure and function: Cardiac structure and function: Histology and retention: | 11 <ul style="list-style-type: none"> • EHT administration almost completely restored FAC • This was not observed with acellular patches or EC-only patches • $11.9 \pm 23.1\%$ of the infarct was remuscularised • Cells were biodistributed to other organs, predominantly the lungs • Ventricular specification of retained hiPSC-CMs • Continued maturation of retained hiPSC-CMs as demonstrated by hiPSC-CM sarcomere length relative to in vitro culture |
| Upscaled EHTs Bovine Fibrin (ogen) | 20×10^6 hiPSC-CMs | Permanent LAD coronary artery ligation with patch applied concurrent to MI. New | 28 days post-administration | Cardiac structure and function: Cardiac structure and function: Histology and retention: | 12 <ul style="list-style-type: none"> • $10.04 \pm 3.1\%$ increase in FAC relative to acellular patch • 3.1% of cells identified within the EHT were hiPSC-CMs • Infiltration of functional host vasculature into the EHT • Reduction in infarct scar size relative to acellular patch |

| | | | | | |
|-----------------------------------------|------------------------------------------------------------------------|----------------------------------------------------------------------------------------------------|----------------------------------------------------------------------------------------------------------------------------------------------------------------------------------------------|-------------------------------------------------------------------------------------------------------------------------------------------------------------------------------------------------------------------------------------------------------------------------------------------------------------------------------------------------------------------------------------------------------------------------------------------------------------------------------------------------------------------------------------------------------------------------------------------------------------------------------------------------------------------------------------------------------------------------------|----|
| | | Zealand white male rabbits | retention: 28 days post-administration | | |
| Clinically-sized EHTs | 40 × 10 ⁶ rhesus macaque iPSC-derived CMs and stromal cells | Chronic heart failure model established 6-month post IRI at which point the patch was administered | Cardiac structure and function: MRI performed 1-, 2-, 3-, and 6-months post-administration Histology and retention: 6 months post-administration | Cardiac structure and function: <ul style="list-style-type: none"> • Dose-dependent increase of LV wall thickness • Three (consistently) and 1 (transiently) of the 6 macaques that received EHTs demonstrated enhanced contractility • Of these four, those receiving 5 EHTs had enhanced LVEF relative to controls and those receiving 2 EHTs Histology and retention: <ul style="list-style-type: none"> • Infiltration of functional host vasculature into the EHT • Retained iPSC-CMs were terminally differentiated • iPSC-CMs were smaller and less mature as evidenced by preferential expression of foetal rather than adult markers | 13 |
| Bovine collagen type I | 40 × 10 ⁶ hiPSC-derived CMs and stromal cells | MI 5 years prior to EHT administration Female patient with HF (NYHA class III) | Cardiac structure and function: Echocardiography conducted at 3-month follow-up Histology and retention: 3 months post-administration of 10 EHTs | Cardiac structure and function: <ul style="list-style-type: none"> • LV end diastolic and systolic volumes were reduced in this single reported patient • LVEF had increased in this single reported patient Histology and retention: <ul style="list-style-type: none"> • Retained hiPSC-CMs were significantly smaller than host CMs • Infiltration of host vasculature into the EHT • Infiltration of macrophages and B and T cells | |
| Fibrin patch EVICEL [®] Fibrin | 700,000 hESC-derived SSEA-1 ⁺ cardiac progenitors | Permanent LAD ligation with patch applied 5 to 7 weeks post-MI Female nude rats | Cardiac structure and function: Echocardiography at baseline, and then monthly until 4 months post-administration Histology and retention: 4-months post-administration | Cardiac structure and function: <ul style="list-style-type: none"> • Increased LVEF 4 months post-administration relative to MI-only • Decreased LVEDV 4 months post-administration relative to MI-only Histology and retention: <ul style="list-style-type: none"> • Increased angiogenesis in the border zone relative to MI-only rats. • No teratoma formation despite delivering hESC-derived progenitor cells • Exogenous cells were not detectable 1-week post-administration | 17 |

| | | | | | |
|---------------------------------------------|------------------------------------------------------------------------------------------------------------------------------|-----------------------------------------------------------------------------------------------------------------------------------------------------------------------------------------------------------------|------------------------------------------------------------------------------------------------------------------------------------------------------------------------------------------------------------------------------------|----------------------------------------------------------------------------------------------------------------------------------------------------------------------------------------------------------------------------------------------------------------------------------------------------------------------------------------------------------------------------------------------------------------------------------------------------------------------------------------------------------------------------------------------------------------------------------------------------------------------------------------------------|----|
| | 5.0 - 10 × 10 ⁶ hESC-derived SSEA-1 ⁺ cardiac progenitors (Median dose: 8.2 × 10 ⁶) | <ul style="list-style-type: none"> • MI >6 months prior to patch administration and an LVEF ≥15% - ≤35%. • 1 female, 5 male • Patch applied underneath a pericardial 'flap' | <p>Cardiac structure and function: Echocardiography at baseline, and then 1, 3, 6, and 12 monthly post-administration. A patient's functional status was also assessed via the 6-min walk test.</p> | <p>Cardiac structure and function:</p> <ul style="list-style-type: none"> • Patients were free from ventricular arrhythmias and cardiac teratoma • Of the 4 patients assessed 12-months post-administration, all 4 had a decrease in NYHA functional class from III to I/II indicative of improved LVEF that improved from 26% to 38.5% (although not statistically significant) • Statistically significant improvement in wall motion underneath where the patch was placed. | 14 |
| ExoGel Hyaluronic acid (HA) hydrogel | 1 × 10 ⁶ MSC-derived exosomes/μl | <p>Transverse aortic constriction (TAC) with patch injection concurrent to HF</p> <p>Rat</p> <p>C57BL/6 mice</p> | <p>Cardiac structure and function: Echocardiography at baseline and 28 days after patch injection</p> <p>Histology and retention: 28-days post-administration (rat) and in-vivo fluorescent tracking (mouse)</p> | <p>Cardiac structure and function:</p> <ul style="list-style-type: none"> • The LV internal diameter at end systole was reduced relative to control rats (HF and PBS) and rats receiving an acellular patch. • LVEF and LVFS were both enhanced by the ExoGel. <p>Histology and retention:</p> <ul style="list-style-type: none"> • Retention of MSC-derived exosomes within the heart was improved when administered via the ExoGel as compared to saline. • ExoGels prevented host CMs from experiencing hypertrophy, reduced CM apoptosis, and enhanced CM proliferation in vivo. | 18 |
| Microneedle patch Gelatine | Exosomes isolated from HUCMSCs and loaded with microRNA-29b (miR-29b) mimics | <p>Permanent LAD ligation with patch applied concurrent to MI</p> <p>Male</p> <p>C57BL/6 mice</p> | <p>Cardiac structure and function: Echocardiography at baseline and 1, 3, 7, 14, and 28 days post-administration</p> <p>Histology and retention: Fibrosis was investigated 28 days post-administration</p> | <p>Cardiac structure and function:</p> <ul style="list-style-type: none"> • Microneedles patches loaded with miR-29b mimic-containing exosomes improved LVEF and LVFS 14 days post-MI relative to MI-only animals and relative to microneedle patches loaded exosomes without miR-29b 28 days post-MI. <p>Histology and retention:</p> <ul style="list-style-type: none"> • Exosome-containing microneedle patches reduced fibrosis and the size of the infarct 28 days post-MI. | 15 |

| | | | | | |
|-------------------------------------------------------|----------------------------------------------------------------------------|-------------------------------------------------------------------------------------------------------------------------------------------------------------------|-----------------------------------------------------------------------------------------------------------------------------------------------------------------------------------------------------------------------------------------------------------------|----------------------------------------------------------------------------------------------------------------------------------------------------------------------------------------------------------------------------------------------------------------------------------------------------------------------------------------------------------------------------------------------------------------------------------------------------------------------------------------------------------------------------------------------------------------------------------------------------------------------------------------------------------------------------------------|----|
| Electrospun nanofibrous patch PCL/ Gelatine | 2 × 10 ⁶ rat bone marrow-derived MSCs/patch | Permanent LAD ligation with patch applied one-week post-MI Sprague Dawley rats Wt1 ^{CreERT2/+} , R2 6 ^{mTmG} transgenic mice (Tg) | Cardiac structure and function: Echocardiography at baseline and 4 weeks post-patch administration Histology and retention: 4 weeks post-patch administration. Lineage tracing of epicardial-derived cells and derivatives (Tg mice) | Cardiac structure and function: <ul style="list-style-type: none"> • Patches containing MSCs improved post-MI LVEF • The MSC-containing patch, in addition to acellular patches, and direct injection of MSCs, enhanced fractional shortening, decreased the scar size, and increased LV wall thickness. Histology and retention: <ul style="list-style-type: none"> • Increased blood and lymphatic vessels • The cell patch group had a greater number of Wt1⁺ EPDCs than patch and MSC-only groups | 19 |
| Bioprinted patch Bovine collagen type I | 1 × 10 ⁵ muscle-derived MSCs (mdMSCs) hiPSC-derived MSCs | IRI model of MI with patch applied 3 weeks post-MI Wistar rats | Cardiac structure and function: Echocardiography 3 weeks post-MI, to determine which rats had reduced LVEF, and 4 weeks after patch administration. Histology and retention: 4 weeks post-administration | Cardiac structure and function: <ul style="list-style-type: none"> • Animals receiving either acellular patches or those seeded with mdMSCs demonstrated a less pronounced change of their LV end systolic volume. • The mdMSC-seeded patch did not prevent post-MI changes in LV end diastolic volume; however, it did increase LVEF. Histology and retention: <ul style="list-style-type: none"> • Neither the acellular patch nor the mdMSC-seeded patch reduced the infarct size • mdMSC-seeded patches reduced the expression of genes associated with apoptosis, inflammation, and HF relative to MI-only animals. | 20 |

BM: Biomaterial; **EHT:** Engineered heart tissue; **FAC:** Fractional area change; **HF:** Heart failure; **hiPSC-CM:** human induced pluripotent stem cell-derived cardiomyocytes; **hiPSC-EC:** human induced pluripotent stem cell-derived endothelial cells; **hESC-CM:** human embryonic stem cell-derived cardiomyocytes; **HUCMSC:** human umbilical cord mesenchymal stem/stromal cell; **HUVEC:** Human umbilical vein endothelial cell; **IRI:** Ischaemia reperfusion injury; **LAD:** Left anterior descending; **LVFS:** Left ventricle fractional shortening; **LVEF:** Left ventricular ejection fraction; **MSC:** Mesenchymal stem/stromal cell; **NYHA:** New York Heart Association HF classification; **EPDCs:** Epicardial-derived cells; **md-MSCs:** muscle-derived MSCs; **LVESV:** LV end-systolic volume; **LVEDV:** LV end-diastolic volume.

Further, the transplanted hearts were devoid of tumour-formation and arrhythmia, illustrating that EHTs could be safely administered to large animal models. These EHTs are currently undergoing clinical assessment^{17,19} and histological examination of an EHT-transplanted heart (Fig. 2Diii) from a patient who subsequently received a heart transplant 3 months post-EHT administration revealed retention of hiPSC-CMs within the EHTs, although they were smaller and relatively less mature compared to adult CMs proximal to the infarct. Despite this retention, subsequent patients will receive 20 EHTs (a total of 800×10^6 hiPSC-derived cells), double the number administered to the evaluated patient.

These EHTs lacked hiPSC-ECs, and capillary density within the EHT was markedly lower than in the host myocardium. Recent pre-clinical investigation in a rat model of MI showed that the concomitant delivery of hiPSC-CMs with established microvessels enhanced their retention.²⁰ Although hiPSC-CMs can be attained at scale, hiPSC-based therapies remain expensive, and their cost-benefit analysis is central to translational viability. Thus, enhanced retention of hiPSC-CMs may allow for fewer initial hiPSC-CMs and EHTs to be delivered, drastically reducing the cost of this therapeutic intervention.

Although EHTs aim to remuscularise the infarcted myocardium through the delivery and retention of viable, adult-like CMs that contribute to LV contractility, pre-clinical studies in rodent models of CHF have shown that irradiated EHTs (devoid of viable cells) achieved outcomes comparable to rats receiving human embryonic stem cell-derived CM (hESC-CM)-containing EHTs. Indeed, LV remodelling was reduced following administration of either EHT; however, this did not enhance post-MI cardiac function,¹⁴ suggesting that either the mechanical support conferred to the LV by the EHT, or the immune response elicited to clear non-viable exogenous cells may also be important to post-MI cardiac repair.

The observation that therapeutic benefits could be attained without directly replacing contractile tissue prompted the evaluation of other hPSC-derived cells. Indeed, hESC-derived cardiac progenitor cells encapsulated within a fibrin patch improved LVEF and attenuated pathological remodelling 4 months post-administration in a rat model of MI, independent of cell retention.²¹ To date, two clinical reports have delivered these fibrin patches (Fig. 2E) during coronary bypass grafting, validating the safety of this approach and the absence of arrhythmia or teratoma formation.^{22,23}

More recently, hiPSC-derived mesenchymal stem/stromal cells (hiPSC-MSCs) have been investigated although, when compared to muscle-derived MSCs (mdMSCs), they exhibited weaker pro-angiogenic and anti-inflammatory effects. As such, mdMSCs were selected for further investigation and encapsulated within bioprinted collagen hydrogels, which attenuated deleterious increases in LV end-systolic volume and significantly enhanced post-MI LVEF in a rat model of IRI. Further, these mdMSC-containing collagen hydrogels downregulated genes associated with apoptosis, heart failure, and inflammation.²⁴

Collectively, these studies demonstrated that biomaterial-based patches containing non-CMs could also yield beneficial effects following MI and have contributed to the establishment of the ‘paracrine hypothesis’²⁵ whereby cells or their derivatives augment cardiac functionality either through the release of factor-rich extracellular vesicles (EVs, particularly exosomes), or the acute immune response they trigger.²⁶

CTE solutions that deliver exosomes

Given longer-term retention of exogenous cells may not be essential to the short-to-medium-term enhancement in post-MI cardiac function, several CTE solutions have been developed to incorporate cellular-derivatives rather than cells themselves. EVs, particularly exosomes, are amongst the most promising. These lipid nanovesicles, released by most cells upon fusion of multivesicular endosomes with the plasma membrane²⁷ release bioactive factors, including proteins, metabolites, and nucleic acids such as messenger and micro RNAs (mRNA and miRNA, respectively), that may augment cardiac remodelling and improve post-MI cardiac function (Table 1).

To this end, hyaluronic acid-based hydrogels loaded with MSC-derived exosomes attenuated adverse cardiac remodelling in a murine model of CHF.²⁷ A more refined strategy focused on identifying the miRNAs within the exosomes that mediate this therapeutic effect.²⁸ As such, mimics of miRNA-29b, known to attenuate post-MI cardiac fibrosis,²⁹ were loaded into MSC-derived exosomes and delivered to the infarcted murine LV on the surface of a gelatine-based microneedle (MN) patch (Fig. 2F). This enabled deeper tissue penetration and delivery of these exosomes into the LV, thereby enhancing their *in vivo* retention, and ultimately enhancing post-MI LVEF.

Recently, miRNA-sequencing analysis of exosomes derived from quiescent macrovascular ECs revealed 561 uniquely expressed immunomodulatory miRNAs that alleviated SARS-CoV-2-mediated cardiac injury by downregulating the toll-like receptor–nuclear factor κ B (TLR–NF- κ B) axis and thus the proinflammatory response to viral infection³⁰ that can lead to myocarditis and MI without obstructive coronary artery disease.³¹ When incorporated into Biowires, EHT-like fibrin-based hydrogels suspended between a pair of poly(octamethylene maleate (anhydride) citrate) (POMaC) wires⁴⁸, endothelial-derived exosomes also enhanced the *in vitro* contractility and force generation capacity of hiPSC-CMs thereby warranting their inclusion and investigation in subsequent cell-free CTE solutions.

As these cell-free strategies do not rely on large-scale delivery of exogenous cells to the infarcted myocardium, they are significantly cheaper and thus more attractive solutions from a clinical translation perspective; however, it remains unclear whether the observed enhancement in cardiac function is maintained longer-term given these strategies do not remuscularise the infarct. Therefore, concomitant delivery of miRNAs that instigate endogenous cardiac regeneration (miR-199a) should also be considered in such CTE solutions.³³

TISSUE-INDUCING BIOMATERIALS

Bioactive molecule-mediated endogenous cardiac repair

Various bioactive molecules, including metabolites, peptides, growth factors, and antibodies have been investigated for endogenous cardiac tissue repair (Table 2). Indeed, a peptide-targeting/biorthogonal conjugation (PBTC) strategy enabled the recruitment of CD34⁺ endothelial progenitor cells (EPCs) towards the heart³⁴. EPCs labelled with azide-PEG-CD34 were recruited toward injured blood vessels *ex vivo*. PBTC treatment increased the proliferation of CMs as well as enhanced the number of blood vessels, and improved cardiac function as evidenced by significantly increased LVEF and FS in a murine model of MI.

Moreover, multivarious bioactive peptides, including stromal cell-derived factor 1 alpha (SDF-1 α) and neuropeptide substance P (SP) are also upregulated following MI, which may have the potential to recruit putative progenitor cells (PCs) for cardiac tissue repair.^{35,36} Beside bioactive cues, polymers with inherent multifunctionality have been shown to promote cardiac tissue repair.

Table 2: Endogenous cardiac tissue repair based on functional biomaterials.

| Biomaterials | Bioactive cue | Observed effect | Functional improvement | Mechanism | Ref. |
|---------------------------------------------------|--------------------------------------|----------------------------------------------------------------------------------------------------------------------------------------------------------------|-------------------------------------------------------------------------------------------------------------------------------|-----------------------------------------------------------------------------------------------------------------------------------------------------------------------------|---------------|
| Peptide-targeting biorthogonal conjugation (PBTC) | CD34 and CD41 antibodies | DBCO-PEG-CD34 improved CD34 cell attachment Azid-PEG-CD41 increased platelet targeting Ki67 ⁺ cells increased; CMs proliferation increased | # of blood vessels increased; LVEF increased | CD34 can target EPCs and CD41 can increase their homing to the myocardium | ³⁵ |
| PPy dispersed into PCNU | / | Conductivity of PCNU increased; MSC growth increased | Alleviated AF in a mice model | Synchronization between patch and host myocardium increased | ³⁶ |
| PGS-PCL and NdFeB-based magnetic cardiac patch | ECs-SPIONS; Ad-SPIONS; and NV-SPIONS | Attachment of ECs-SPIONS; Ad-SPIONS; and NV-SPIONS increased | Number of capillaries and arterioles increased; integration with host vasculature increased; and LVEF and LVFS increased | Increased accumulation of ECs-SPIONS <i>in vitro</i> and <i>in vivo</i> | ⁴⁰ |
| PPC star-shaped PEG-maleimide-based hydrogels | Citrate and MYDGF | Sustained release of BSA for up to 144 h and increased tubule-like network formation of HUVECs | LVEF and LVFS increased; LVIDs and LVIDd slightly increased; myocardial viability increased, and fibrosis decreased | MYDGF-induced increase in angiogenesis of HUVECs as well as multifunctional benefits of citrate | ⁴² |
| Poly(citrate-co-itaconate) (PICO) | Citrate (CA) and itaconate (ITA) | Beating frequency of CMs increased, CA and ITA were released in a sustained fashion | Fewer CD68 ⁺ while increased CD206 ⁺ cell infiltration in the patches implanted on a healthy epicardium | CA- and ITA-mediated ROS scavenging and hypoxia alleviation; CA can induce inflammation resolution via Ca ²⁺ -citrate complex formation; and ITA can inhibit SDH | ⁴³ |
| d-ECM/GP-based hydrogels | Glycopeptide | Macrophages polarization toward M2 phenotype increased' Tube formation of HUVECs increased | LV wall thickness increased, LV wall stress decreased, and LVEF remained preserved | Immune cell recognition via mannose (CD206) receptors | ⁴⁴ |

| | | | | | |
|---------------------------------------------------------|--------------------------------------------------------|----------------------------------------------------------------------------------------------------------------------------------------------------------|----------------------------------------------------------------------------------------------------------------|-----------------------------------------------------------------------|---------------|
| h-d-ECM/HA-Tyramine hydrogels | HA-tyramine to increase tissue adhesion | Robust adhesion with porcine myocardium, ECs and CMs survival was increased, and CD34 ⁺ and α -SMA ⁺ vessels were increased | Higher LV wall thickness, Reduced fibrosis, and increased LVESD | HA-Tyramine mediate enhanced adhesion with myocardium | ⁴⁵ |
| GelMA hydrogel blended with micro (μ -solar cells) | μ -solar cells can induce optoelectric stimulation | Viability of hiPSC-CMs and rat CMs increased; Sarcomeric α -actinin, Connexin 43, and Troponin T expression increased | Synchronization ability of tissue was modulated with optoelectric stimulation, beating frequency was increased | μ -solar cells can induce optoelectronic stimulation of the heart | ⁴¹ |

PBTC: Peptide-targeting biorthogonal conjugation; **DBCO:** dibenzylcyclooctyne; **LVEF:** left ventricular ejection fraction; **CMs:** cardiomyocytes; **EPCs:** endothelial progenitor cells; **FMhMSCs:** MSC from fetal membranes of term placenta; Human cardiac-derived progenitor cells; **PPy:** polypyrrole; **PCNU:** PPy-dispersed polycarbonate urethane; **AF:** Arterial fibrillation; **PGS-PCL:** polyglycerol sebacate-polycaprolactone; **ECs-SPIONS:** super paramagnetic iron oxide endothelial cells; **NV-SPIONS:** super paramagnetic iron oxide-labelled neovesicles; **Ad-SPIONS:** super paramagnetic iron oxide-labelled adenovirus; **H₂O₂:** hydrogen peroxide; **EF:** ejection fraction; **FS:** fractional shortening; **ESV:** end-systolic volume; **EDV:** end-diastolic volume; **α -SMA:** alpha smooth muscle actin; **PPC:** poly(PEG-Co-citrate); **BSA:** bovine serum albumin; **PEG:** polyethylene glycol; **HUVECs:** human umbilical vein endothelial cells; **LVIDs:** systolic left ventricular internal dimension; **LVIDd:** diastolic left ventricular internal dimensions; **PICO:** poly(citrate-co-itaconate); **CA:** citrate; **ITA:** itaconate; **SDH:** succinate dehydrogenase; **d-ECM:** decellularized extracellular matrix; **GP:** glycopeptide; **LVESD:** left ventricular end-systolic diameter; **Gel-MA:** methacrylated gelatin; **hiPSC-CMs:** human induced pluripotent stem cell-derived cardiomyocytes.

Functional polymer-mediated endogenous cardiac repair

Intrinsically functional biomaterials

The post-MI fibrotic scar has different impedance and conductance relative to the healthy myocardium, which can promote arrhythmogenesis and increase the risk of sudden cardiac death. Inorganic nanomaterials and conducting polymers may offer a solution.⁵⁸ Indeed, nanoparticles (NPs) derived from polypyrrolle (PPy) have been integrated into polycarbonate polyurethane (PCNU) fibres. This PPy-PCNU patch was evaluated in a rat model of induced atrial fibrillation where it restored electrical signalling conduction quicker than PCNU-only fibres thus potentially providing a solution to the electrical disturbance within the LV following MI.³⁷

Magnetic cardiac patches derived from polyglycerol sebacate-polycaprolactone (PGS-PCL) and a neodymium magnet (NdFeB) can also be placed on the infarcted LV of rats where they can recruit superparamagnetic iron oxide-labelled-ECs that remain viable on the patch and form a functional vasculature.³⁸ Magnetic patches containing these ECs reduced LV scar size whilst increasing LV wall thickness and improving post-MI LVEF.

Functional scaffolds with optoelectronic ability have been shown to modulate the beating of human and rat CMs *in vitro*, as well as rat CMs *in vivo*.³⁹ Briefly, micro-solar cells were mixed with methacrylated gelatine and used to 3D print scaffolds. hiPSC-CMs or rat CMs were seeded onto these scaffolds where they remained viable for up to 2 weeks. Given that coordinated beating of engineered cardiac tissue constructs with the host myocardium is vital to attaining a regenerated functional myocardium that is not pro-arrhythmogenic, the ability of the optoelectronically active scaffold to synchronise with the myocardium was evaluated revealing that the beating of the rat heart could be modulated via pulsed light.

Biomaterials releasing regenerative cues

Biomaterials can also be engineered to release functional cues to stimulate cardiac regeneration. For example, poly(polyethylene glycol-*co*-citrate) (PPC)-based hydrogels enabled the controlled release of citrate (CA) and myeloid-derived growth factor (MYDGF).⁴⁰ The *in vitro* tube formation capacity of HUVECs was enhanced in these

MYDGF-loaded hydrogels, a finding that was mirrored *in vivo* with upregulated neovascularisation of the infarct coupled with a reduced scar size and improved LVEF in a mouse model of MI. Other citrate containing biomaterials including poly(citrate-co-itaconate) (PICO) can release itaconate (ITA) in addition to CA. Both of these factors have been shown to be cardio-protective and prevent hiPSC-CM apoptosis whilst retaining CM beating following *in vitro* IRI.⁴¹ When evaluated *in vivo* within healthy rats, patches containing a high content of CA and ITA modulated the foreign body immune response, as evidenced by minimal infiltration of CD68⁺ macrophages and the absence of a pronounced fibrotic capsule, thereby demonstrating their robust biocompatibility.

Approaches based on decellularised extracellular matrix

Decellularised extracellular matrix (d-ECM) has also been widely investigated for endogenous cardiac tissue repair owing to its ability to recapitulate the native ECM architecture and potentially present bioactive cues. However, the decellularisation process can also remove or denature such cues whilst also exposing collagen fibres that can be pro-inflammatory. Polysaccharides and glycopeptides (GP) can be harnessed as they resemble proteoglycans (PGs), including heparan sulphate (HS) and chondroitin sulphate (CS). Kong et al. fabricated dECM/GP-based hydrogels, which exhibited stiffness comparable to cardiac tissue alongside a microporous structure that promoted cell infiltration and angiogenesis.⁴² d-ECM/GP hydrogels enhanced EC migration and induced macrophage polarisation towards a pro-reparative M2 phenotype, which produced more vascular endothelial growth factor (VEGF) and supported EC viability. These patches also attenuated LV remodelling in a rat model of MI. The d-ECM can be further modified with adhesive cues, e.g., hyaluronic acid-tyramine (HA-Ty) and recombinant tyrosinase from streptomyces avermitilis (SA-Ty) to obtain pdHA-t that robustly adheres to the myocardium (0.78 ± 0.08 kPa) whilst also supporting and retaining viable hESC-CMs and -ECs.⁴³ These hydrogels were evaluated in a rat model of MI resulting in enhanced angiogenesis, reduced scar size, and improved functional parameters including LVEF and LVFS.

Self-assembling peptides

More recently, self-assembling peptides have been studied for cardiac tissue repair. The

structure and function of peptide nanofibers can be tuned, and ECM-derived signals or functional peptide units can be engineered into peptide nanofibers to further widen their pro-angiogenic potential or ability to adhere cells. Indeed, glycosaminoglycans-mimetic self-assembling peptide fibres can attenuate adverse cardiac remodelling in a rat model of MI.⁴⁴ Moreover, these GAGs-mimetic peptide fibres increased the number of arteries and capillaries both in the infarct and peri-infarct area, demonstrating a 2.7-fold increase in α -SMA⁺ vessels and a 1.6-fold increase in rat endothelial cell antigen-1 (RECA-1⁺) vessels alongside higher gene expression of RECA-1 and angiopoiten-1 (Ang-1).

CYTOKINE/CHEMOKINE-MEDIATED ENDOGENOUS CARDIAC REPAIR

Alongside biomaterials, multivarious cytokines and chemokines can be harnessed to induce cardiac tissue repair (Table 3). The immunomodulatory drug Fingolimod (FTY720) was delivered to the infarcted heart via a hydrogel fabricated from the functional polypeptide mPEG-poly(L-methionine₂₀-co-L-alanine₁₀) (PMA). L-methionine, an antioxidant component of PMA, can scavenge ROS through its thioether side chain and alter the hydrophobicity of the polymer to induce FTY720 release via gel-to-sol transition. The resultant patch was evaluated in both a rat and rabbit model of IRI resulting in enhanced post-MI LVEF in both models. Further, the patch enabled synergistic anti-apoptotic and anti-inflammatory effects whilst also scavenging ROS, promoting macrophage polarisation towards the M2 phenotype, and attenuating LV remodelling.⁴⁵

Table 3. Endogenous cardiac tissue repair based on biomaterials and/or cytokines and chemokines.

| Delivery vehicle | Payload | Observed effects | Functional improvement | Mechanism | Ref. |
|--------------------------------------------------------------------|---------------------------------------------------------|------------------------------------------------------------------------------------------------------------------------------------------|----------------------------------------------------------------------------------------------------------------------------------------------------------------------------|-------------------------------------------------------------------------------------------------------------------|------|
| mPEG-Poly(L-methionine ₂₀ -co-L-alanine ₁₀) | FTY720 I/R model and Rabbit and swine I/R model | CMs apoptosis decreased, ROS scavenging increased, M1 to M2 polarization increased, Arg/iNOS ratio increased | LVEF increased, CMs hypertrophy decreased, Fibrosis decreased, cardiac function increased, and CD31 ⁺ vessel density increased | L-methionine is an active component of polymer, which can increase ROS scavenging | 47 |
| PLGA microneedles | VEGF | Rapid release of VEGF enhanced vascularization, and sustained release of exosomes | CD31 ⁺ vessel density increased, and α -SMA ⁺ vessel density increased in a human cardiac organoid (HCO) model | VEGF can promote neovascularization, and exosomes can induce endogenous cardiac tissue regeneration | 48 |
| SDF-1 α -modified collagen hydrogels | Collagen-binding domain (CBD)-conjugated SDF-1 α | Binding of HSCs and MSCs increased in CBD-SDF-1 α -loaded collagen hydrogels Recruitment of c-kit ⁺ cells increased | Neovascularization increased and cardiac function increased in an MI model | CBD-SDF-1 α can efficiently bind to collagen hydrogels and extend the half-life of SDF-1 α | 33 |
| Self-assembling peptide-based hydrogels | Ac-SDKP and SDF-1 α | / | / | Thymosin β -4-derived Ac-SDKP can increase neovascularization, while SDF-1 α can improve cell homing | 49 |
| Collagen type I hydrogel | HDA7-derived 7 amino acids peptide Rat MI model | Micro vessel formation increased, Stem cell antigen-1 (Sca-1 ⁺) cells increased, and cell apoptosis decreased | In an MI model, cell cycle progression was increased, Sca-1 ⁺ cells were co-localized with CD31 & Ki67 ⁺ cells with Troponin-T ⁺ cells | HDA7-derived 7 amino acids peptide can increase the recruitment of Sca-1 ⁺ cells | 50 |
| PCL/Col-I cardiac patch | SP and IGF-1C-derived peptide | CD29 ⁺ stromal-like cell recruitment increased; TUNEL ⁺ cells decreased | LV wall thickness increased; Vascularization increased in a mice MI | SP can recruit endogenous stromal-like cells, while IGF-1C-derived peptide can suppress CMs apoptosis | 51 |

| model | | | | |
|-----------------------------------------------------|-----------------------------------------------------------|-----------------------------------------------------------------------|----------------------------------------------------------------------------------------------------------------------------------------------------------------------------------------------------|---------------------------------------------------------------------------------------------------------|
| Tyramine-alginate conjugated silk fibroin hydrogels | Oxygen-producing microparticles (OMPs) and SDF-1 α | Beating frequency of iPSCs-CMs increased; Cell apoptosis decreased | C-kit ⁺ cells and CD34 ⁺ cells increased; LV, LVSV, and LVDV increased | OMPs can provide oxygen to increase vascularization while SDF-1 α can recruit SPCs ⁵² |
| Thermo-sensitive hydrogels | DPCA | HIF-1 α increased | stabilization Cardiac function increased in an MI model No. of PH3 ⁺ and ki67 ⁺ cells increased CX43 expression increased Fibrosis and apoptotic cells decreased | DPCA can increase HIF-1 α stabilization as well as improve vascularization ⁵⁸ |

FTY720: Fingolimod; **I/R**: ischemia-reperfusion; **CMs**, cardiomyocytes; **ROS**: reactive oxygen species; **Arg**: arginase; **iNOS**: inducible nitric oxide synthase; **LVEF**: left ventricular ejection fraction; mPEG45-P(Met₂₀-co-Ala₁₀): methoxy poly(ethylene glycol)₄₅-poly(L-methionine₂₀-co-L-alanine₁₀); **PLGA**: poly(lactic-co-glycolic acid); **VEGF**: vascular endothelial growth factor; **α -SMA**: alpha smooth muscle actin; **SDF-1 α** : stromal cell-derived factor 1 alpha; **CBD**: collagen-binding domain; **HSCs**: hematopoietic stem cells; **MSCs**: mesenchymal stem cells; **Ac-SDKP**: N-acetyl-Seryl-Aspartyl-Lysyl-Proline; **HDA7**: Histone deacetylase 7; **Sc α -1⁺**: stem cell antigen-1; **MI**: myocardial infarction; **PCL/Col-I**: polycaprolactone/collagen type I; **SP**: neuropeptide substance P; **IGF-1C**: Insulin-like growth factor 1 domain C; **TUNEL**: Terminal deoxynucleotidyl transferase dUTP nick end labelling; **OMPs**: Oxygen-producing microparticles; **iPSCs-CMs**: induced pluripotent stem cell-derived cardiomyocytes; **LV**: left ventricular; **LVSV**: left ventricular systolic volume; **LVDV**: left ventricular diastolic volume; **SPCs**: stem/progenitor cells; **DPCA**: 1,4 dihydro phenanthroline-4-one-3 carboxylic acid; **HIF-1 α** : hypoxia-inducible factor 1 alpha; **CX43**: Connexin 43.

Growth factors and exosomes can also be simultaneously utilised to address MI-mediated acidolysis and inflammation. Indeed, VEGF was encapsulated into liposomes and loaded into the base of a MN patch to facilitate early vascular network formation. On the other hand, MSC-derived exosomes were click-coated to egg-shell protein and loaded into the MNs. These exosome-loaded NPs disintegrated at a lower pH and were self-propelled into cardiac tissues. MNs co-loaded with exosomes and VEGF enabled the greater production of CD31⁺ vessels and α -SMA⁺ arterioles in both an *in vitro* human cardiac organoid model and a rat model of acute MI.⁴⁶

The mobilisation and recruitment of stem/progenitor cells (SPCs) has also been suggested as a promising approach for cardiac tissue repair. Bioactive peptides, including SDF-1 α can be upregulated after MI, and help promote revascularisation of ischaemic tissue due in part to SPCs mobilisation and recruitment.⁴⁷ Nonetheless, the expression of cytokines/chemokines is rapidly levelled off *in vivo*, thereby reducing the effectiveness of this approach. Alternative approaches such as viral and non-viral vectors, protein delivery, and therapeutic peptide administration are therefore required to upregulate and maintain their expression for longer time periods. Indeed, the collagen-binding domain (CBD) has been conjugated with the C-terminus of SDF-1 α , an approach that facilitated the strong binding of SDF-1 α to collagen hydrogels *in vitro*, thereby enabling sustained and controlled release of SDF-1 α . This upregulated its capacity to bind more hematopoietic stem cells and MSCs.⁴⁸ Briefly, CBD-SDF-1 α elevated the mobilisation and recruitment of C-kit⁺ cells in an acute rat model of MI and improved neovascularisation, as evidenced by significantly higher capillary density, as well as LVFS and LVEF.

Similarly SDF-1 α has been used in conjunction with Ac-SDKP (N-acetyl-seryl-aspartyl-lysyl-proline) for improved stem cell homing, angiogenesis and enhanced cardiac regeneration in a rat chronic rat model of MI.⁴⁹ The SDF-1 α peptide was physically incorporated into a hyaluronic acid-based hydrogel, and its degradation was dependent on hydrogel degradation, whilst Ac-SDKP was covalently immobilised onto the hydrogel. Zhang et al. loaded histone deacetylase (HDAC)7-derived peptide into collagen type 1 (Col I) hydrogels, which increased microvessel formation, enhanced the recruitment and differentiation of stem cell antigen (Sca)-1⁺ cells, reduced cell apoptosis, and promoted CM cell cycle progression in a mouse model of MI.⁵⁰ More importantly, Sca-1⁺ cells were co-

localised with CD31⁺ cells, whilst Ki67⁺ cells were co-localised with cardiac troponin T expressing cells.

Oxygen-producing biomaterials may help alleviate the post-MI ischemic microenvironment, and they can additionally modulate the function of SPCs. For instance, oxygen-producing microparticles (OMP) improved the survival and metabolic function of HUVECs *in vitro*.⁵¹ The combined delivery of OMP and SDF-1 α in tyramine-alginate conjugated silk fibrin hydrogels also enhanced the beating rate of hiPSCs-CMs whilst decreasing cell apoptosis and scar size in a rat model of MI. Further, this strategy enhanced post-MI LVEF and attenuated remodelling as evidenced by reduced LV systolic and diastolic volumes. Similarly, an antioxidative polyurethane patch containing calcium peroxide (CaO₂) was electrospun over a collagen sheet and adipose-derived stem cell exosomes were subsequently absorbed on the patch. These patches enhanced the survival and proliferation of H9C2 cardiac cells, promoted the *in vitro* tube formation capacity of HUVECs, and reduced both oxidative stress and the scar size 8 weeks post-implantation in a rat model of MI.⁵²

Substance P (SP) is an 11-amino acid peptide, which can interact with neurokinin 1 receptors on SPCs to mobilise and recruit them toward injured tissues. SP levels are thought to increase following ischemic injury³⁶ however, this is transient with expression levels quickly returning to basal levels.^{53,54} In turn, PCL/Col I-based cardiac patches were co-loaded with SP and insulin-like growth factor (IGF)-1C domain-derived peptide (GYGSSRRAPQT). These patches recruited CD29⁺ stromal-like cells and limited cell apoptosis⁵⁵ IGF-1C/SP-loaded patches improved LV wall thickness and vascularisation whilst also reducing fibrosis and thus the scar size. SP-mediated amelioration of cardiac dysfunction can be ascribed to SPCs recruitment and inflammation resolution.^{56,57}

Zhu and colleagues covalently conjugated DPCA with N-isopropylacrylamide (NIPAM)-based thermo-sensitive hydrogels, which not only enabled non-covalent interaction among adjacent DPCA units but also showed zero-order release kinetics due to hydrolysis of the ester bond, autocatalysis by MA units, and hydrophilicity.⁵⁸ These hydrogels stabilised hypoxia-inducible factor 1-alpha (HIF-1 α) and significantly ameliorated cardiac functional decline in a rat model of MI as evidenced by increased LVEF and enhanced angiogenesis. DPCA releasing hydrogels also increased the number of proliferating (pH3⁺ and Ki67⁺) cells,

enhanced the expression of connexin 43 (Cx43), whilst decreasing fibrosis and cell apoptosis.⁵⁹ Moreover, stimuli-responsive moieties can be included in the polymer structure and photo-crosslinking can be harnessed to modulate the release profile of the drug. For instance, DPCA-conjugated methacrylated hyaluronic acid hydrogels (HAMA) were first photo-crosslinked, and subsequently non-covalently crosslinked with carboxylated calixarene (CSAC4A). Hydrogels containing disulphide bonds scavenged 75% of ROS, improved HIF-1 α stability, enhanced cardiac function and neovascularisation, and suppressed the proliferation of fibroblasts. Intriguingly, the sustained release of DPCA was more effective relative to the burst release. Therefore, prolonged pharmacological induction of hypoxic signalling through biomaterial-based administration may have also have potential for endogenous cardiac tissue repair.

Discussion

A myriad of strategies have been pursued to stimulate endogenous cardiac tissue repair. Biomaterials with intrinsic functionalities, such as anti-oxidative moieties, angiogenic properties, and cell recruitment cues can promote regeneration by scavenging ROS, promoting CM proliferation, or inducing vascularisation.^{39,40,47,60} Beyond these effects, biomaterials may offer mechanical support to the injured myocardium post-MI, promote positive remodelling, and serve as carriers for bioactive cargos such as EVs or other components of the cell secretome.⁶¹ The molecular mechanisms underlying these effects however remain incompletely understood. Advancements are warranted to develop multi-functional, spatiotemporally controlled therapies that precisely regulate immune responses and regenerative signalling, including the delivery of cell-derived products and exosomes.⁶² In fact, ECM-modulatory proteins (MMPs, TIMP-3) and cardiac-specific miRNAs have shown promise in improving cardiac function in MI models.⁶³

Significant progress has also been made in CTE-based delivery systems, including EHTs, cardiac patches, and exosomes/EVs. Nonetheless, limited survival and retention of cells during *in vitro* culture and post-transplantation *in vivo* remain major hurdles, necessitating alternative strategies to enhance cell survival and deepen mechanistic understanding of

cardiac repair. Among these, MSC-based strategies may offer promising opportunities due to their immunomodulatory and paracrine properties.²⁴ Further research on multifunctional biomaterials is required to translate these advancements into clinically effective therapies.

To complement these advances, studies focused on the biology of heart regeneration should be prioritised. Complete cardiac regeneration has been demonstrated in zebrafish and neonatal hearts.⁹² Stimulating endogenous repair and *in situ* manipulation of cardiac cells may promote CM dedifferentiation and proliferation, potentially eliminating the need for transplantation. Indeed, cell cycle regulators, cyclin-dependent kinases, and non-coding RNAs have been shown to reinitiate CM proliferation.⁶⁴ Epigenetic mechanisms may also offer promising avenues for heart regeneration.⁶¹ Identifying cardiac-inducing bioactive cues, such as peptides, proteins, small-molecule compounds, and stem cell-recruiting factors, remains a key goal. For instance, microRNA (miRNA) delivery has improved cardiac function in preclinical models.⁶⁵ Additionally, short interfering RNA (siRNA)-mediated silencing of von Willebrand Factor (vWF) has mitigated endothelial cell dysfunction *in vitro* without compromising cell viability or growth.⁶⁶ These findings underscore the importance of optimising nucleic acid delivery using intelligent carriers and further elucidating their mechanisms of action.⁶⁷⁻⁶⁹

From a cell-based CTE perspective, the ongoing BioVAT-HF phase 1/2 trial evaluating EHTs will provide vital insight into the therapeutic potential of delivering large numbers of hiPSC-CMs to HFrEF patients. Despite promising preclinical data, long-term retention of transplanted cells remains low prompting a shift towards cell-aggregate models to improve retention and engraftment.⁸ The results of the BioVAT-HF trial will help define the minimum effective cell number, the ideal cellular composition (e.g., inclusion of ECs), and the duration of therapeutic benefit.

This question of durability also underpins a broader distinction between cell-based and cell-free CTE strategies. Whilst exosome-loaded biomaterials and bioactive scaffolds have restored cardiac function in pre-clinical MI and HFrEF models, their benefits are often indirect – via angiogenesis, immunomodulation, and attenuation of adverse remodelling. Only a subset of these approaches stimulate proliferation of endogenous CMs, which is essential for restoring contractility without exogenous hiPSC-CM delivery. Clinical studies

are thus needed to determine whether these effects translate to sustained improvements in cardiac function.

Timing is also critical for exosome-based interventions.⁷⁰ A case report from the ongoing SECRET-HF phase 1 trial showed that EVs derived from hiPSC-CPCs can be administered safely to patients with advanced HFrEF, with preliminary results from a single patient indicating improved LVEF and no adverse effects.⁷¹ If consistent across all 12 enrolled patients, subsequent trials could investigate pairing these EVs with hydrogels or microneedle-based delivery systems to enhance retention and efficacy.

In summary, despite major advances in cell-based⁷² and cell-free CTE strategies, long-lasting beneficial clinical effects have not yet been achieved. Future efforts should integrate advanced biomaterials, optimise delivery systems, and harness endogenous repair mechanisms. A multidisciplinary approach combining developmental biology, bioengineering, and regenerative medicine will be essential for unlocking the full potential of CTE approaches in cardiac regeneration.

Acknowledgment: This work was partially supported by Sigrid Jusélius Foundation, the Finnish Foundation for Cardiovascular Research, and European Union's Horizon Europe research and innovation programme under Marie Skłodowska-Curie grant agreement [101126611].

CRedit Author Statement: **Shafiq M:** Writing – original draft, Writing – review & editing, Methodology, Investigation, Formal analysis, Data curation, Conceptualization; **Majid Q.A.:** Writing – original draft, Writing – review & editing, Formal analysis, Validation, Investigation, Methodology. **Rafique M:** Writing – review & editing, Formal Analysis, Software; **Talman V.,** Resources, Project administration, Funding acquisition, Conceptualization, Writing - review & editing.

Conflict of Interest: The authors declare that they have no known competing financial interests or personal relationships that could have appeared to influence the work reported in this paper.

References

1. Rosano GMC, Seferovic P, Savarese G, et al. Impact analysis of heart failure across European countries: An ESC-HFA position paper. *ESC Heart Fail* 2022;9(5):2767–2778;
2. Koh AS, Tay WT, Teng THK, et al. A comprehensive population-based characterization of heart failure with mid-range ejection fraction. *Eur J Heart Fail* 2017;19(12):1624–1634;
3. Bergmann O, Bhardwaj RD, Bernard S, et al. Evidence for cardiomyocyte renewal in humans. *Science* 2009;324(5923):98–102;
4. Bergmann O, Zdunek S, Felker A, et al. Dynamics of cell generation and turnover in the human heart. *Cell* 2015;161(7):1566–1575;
5. Talman V, Ruskoaho H. Cardiac fibrosis in myocardial infarction—from repair and remodeling to regeneration. *Cell Tissue Res* 2016;365(3):563–581;
6. Majid QA, Fricker ATR, Gregory DA, et al. Natural biomaterials for cardiac tissue engineering: A highly biocompatible solution. *Front Cardiovasc Med* 2020;7:554597;
7. Cui H, Liu C, Esworthy T, et al. 4D physiologically adaptable cardiac patch: A 4-month in vivo study for the treatment of myocardial infarction. *Sci Adv* 2020;6(26):eabb5067;
8. Majid QA, Pandey P, Bellahcene M, et al. Melt electrowritten medium chain length polyhydroxyalkanoate cardiac patches for post-MI cardiac regeneration. *Mater Today Bio* 2025;34:102256;
9. Litviňuková M, Talavera-López C, Maatz H, et al. Cells of the adult human heart. *Nature* 2020;588(7838):466–472;
10. Tiburcy M, Hudson JE, Balfanz P, et al. Defined engineered human myocardium with advanced maturation for applications in heart failure modeling and repair. *Circulation* 2017;135(19):1832–1847;
11. Weinberger F, Breckwoldt K, Pecha S, et al. Cardiac repair in guinea pigs with human engineered heart tissue from induced pluripotent stem cells. *Sci Transl Med* 2016;8(363):363ra148;
12. Jabbour RJ, Owen TJ, Pandey P, et al. In vivo grafting of large engineered heart tissue patches for cardiac repair. *JCI Insight* 2021;6(15):e144068;
13. Jebran AF, Seidler T, Tiburcy M, et al. Engineered heart muscle allografts for heart repair in primates and humans. *Nature* 2025;639(8054):503–511;
14. Menasché P, Vanneaux V, Hagege A, et al. Transplantation of human embryonic stem cell-derived cardiovascular progenitors for severe ischemic left ventricular dysfunction. *J Am Coll Cardiol* 2018;71(4):429–438;

15. Yuan J, Yang H, Liu C, et al. Microneedle patch loaded with exosomes containing microRNA-29b prevents cardiac fibrosis after myocardial infarction. *Adv Healthc Mater* 2023;12(13):e2202959;
16. Riegler J, Tiburcy M, Ebert A, et al. Human engineered heart muscles engraft and survive long term in a rodent myocardial infarction model. *Circ Res* 2015;117(8):720–730;
17. Bellamy V, Vanneaux V, Bel A, et al. Long-term functional benefits of human embryonic stem cell-derived cardiac progenitors embedded into a fibrin scaffold. *J Heart Lung Transplant* 2015;34(9):1198–1207;
18. Cheng G, Zhu D, Huang K, et al. Minimally invasive delivery of a hydrogel-based exosome patch to prevent heart failure. *J Mol Cell Cardiol* 2022;169:113–121;
19. Wang Q-L, Wang H-J, Li Z-H, et al. Mesenchymal stem cell-loaded cardiac patch promotes epicardial activation and repair of infarcted myocardium. *J Cell Mol Med* 2017;21(9):1751–1766;
20. Guesdon R, Santoro S, Cras A, et al. Repair of infarcted myocardium by skeletal muscle-derived mesenchymal stromal cells delivered by a bioprinted collagen patch. *Stem Cell Res Ther* 2025;16(1):427;
21. Brown RD, Ambler SK, Mitchell MD, Long CS. The cardiac fibroblast: Therapeutic target in myocardial remodeling and failure. *Annu Rev Pharmacol Toxicol* 2005;45:657–687;
22. Talman V, Kivelä R. Cardiomyocyte–endothelial cell interactions in cardiac remodeling and regeneration. *Front Cardiovasc Med* 2018;5:101;
23. Fung DG, Chen C, Bilek MMM. Emerging avenues to restore the regenerative capacity of adult mammalian heart. *Front Bioeng Biotechnol* 2022;10:872044.
24. Saxena A, Russo I, Frangogiannis NG. Inflammation as a therapeutic target in myocardial infarction: Learning from past failures to meet future challenges. *Transl Res* 2016;167(1):152–166;
25. Ensminger S, Kutschka I, Brandenburg S, et al. (131)-Two-center surgical experience from the first-in-human BioVAT-HF-DZHK20 Clinical Trial. *J Hear Lung Transplant* 2025;44(4):S64–S65;
26. Sun X, Wu J, Mourad O, et al. Microvessel co-transplantation improves poor remuscularization by hiPSC-cardiomyocytes in a complex disease model of myocardial infarction and type 2 diabetes. *Stem Cell Reports* 2025;20(2):102394;
27. Menasché P, Vanneaux V, Fabreguettes J-R, et al. Towards a clinical use of human embryonic stem cell-derived cardiac progenitors: A translational experience. *Eur Heart J* 2015;36(12):743–750;
28. Hodgkinson CP, Bareja A, Gomez JA, et al. Emerging concepts in paracrine mechanisms in regenerative cardiovascular medicine and biology. *Circ Res* 2016;118(1):95–107;

29. Vagnozzi RJ, Maillet M, Sargent MA, et al. An acute immune response underlies the benefit of cardiac stem cell therapy. *Nature* 2020;577(7790):405–409;
30. Xue Y, Fan X, Yang R, et al. MiR-29b-3p inhibits post-infarct cardiac fibrosis by targeting FOS. *Biosci Rep* 2020;40(9):BSR20201227;
31. Lu RXZ, Rafatian N, Zhao Y, et al. Cardiac tissue model of immune-induced dysfunction reveals the role of free mitochondrial DNA and the therapeutic effects of exosomes. *Sci Adv* 2024;10(13):eadk0164;
32. Conceição AM, Pereira CAC, Rahal MJ, et al. COVID-19 myocarditis mimicking ST-segment elevation myocardial infarction. *Arq Bras Cardiol* 2022;119(3):480–484;
33. Zhao Y, Rafatian N, Feric NT, et al. A Platform for Generation of Chamber-Specific Cardiac Tissues and Disease Modeling. *Cell* 2019;176(4):913–927.e18;
34. Gabisonia K, Prosdocimo G, Aquaro GD, et al. MicroRNA therapy stimulates uncontrolled cardiac repair after myocardial infarction in pigs. *Nature* 2019;569(7756):418–422;
35. Li Z, Shen D, Hu S, et al. Pretargeting and bioorthogonal click chemistry-mediated endogenous stem cell homing for heart repair. *ACS Nano* 2018;12(12):12193–12200;
36. Renko O, Tolonen AM, Rysä J, et al. SDF1 gradient associates with the distribution of c-Kit⁺ cardiac cells in the heart. *Sci Rep* 2018;8(1):1160;
37. Amadesi S, Reni C, Katare R, et al. Role for substance p-based nociceptive signaling in progenitor cell activation and angiogenesis during ischemia in mice and in human subjects. *Circulation* 2012;125(14):1774–1786, s1-19;
38. Deng K, Hua Y, Gao Y, et al. Thermosensitive hydrogel with programmable, self-regulated HIF-1 α stabilizer release for myocardial infarction treatment. *Adv Sci (Weinh)* 2024;11(43):e2408013;
39. Fadle Aziz MR, Wlodarek L, Alibhai F, et al. A polypyrrole-polycarbonate polyurethane elastomer alleviates cardiac arrhythmias via improving bio-conductivity. *Adv Healthc Mater* 2023;12(17):e2203168;
40. Qian B, Shen A, Huang S, et al. An intrinsically magnetic epicardial patch for rapid Vascular reconstruction and drug delivery. *Adv Sci (Weinh)* 2023;10(36):e2303033;
41. Ershad F, Rao Z, Maharajan S, et al. Bioprinted optoelectronically active cardiac tissues. *Sci Adv* 2025;11(4):eadt7210;
42. Yuan Z, Tsou Y-H, Zhang X-Q, et al. Injectable citrate-based hydrogel as an angiogenic biomaterial improves cardiac repair after myocardial infarction. *ACS Appl Mater Interfaces* 2019;11(42):38429–38439;

43. Bannerman D, Pascual-Gil S, Campbell S, et al. Itaconate and citrate releasing polymer attenuates foreign body response in biofabricated cardiac patches. *Mater Today Bio* 2024;24:100917;
44. Kong P, Dong J, Li W, et al. Extracellular matrix/glycopeptide hybrid hydrogel as an immunomodulatory niche for endogenous cardiac repair after myocardial infarction. *Adv Sci (Weinh)* 2023;10(23):e2301244;
45. Lee J, Lee SG, Kim BS, et al. Paintable decellularized-ECM hydrogel for preventing cardiac tissue damage. *Adv Sci (Weinh)* 2024;11(21):e2307353;
46. Rufaihah AJ, Yasa IC, Ramanujam VS, et al. Angiogenic peptide nanofibers repair cardiac tissue defect after myocardial infarction. *Acta Biomater* 2017;58:102–112;
47. Luo Q, Li Z, Sun W, et al. Myocardia-injected synergistically anti-apoptotic and anti-inflammatory poly(amino acid) hydrogel relieves ischemia-reperfusion injury. *Adv Mater* 2025;37(11):e2420171;
48. Wang F, Xu Z, Zheng F, et al. Cardiac organoid model inspired micro-robot smart patch to treat myocardial infarction. *Adv Mater* 2025;37(26):e2417327;
49. Song M, Jang H, Lee J, et al. Regeneration of chronic myocardial infarction by injectable hydrogels containing stem cell homing factor SDF-1 and angiogenic peptide Ac-SDKP. *Biomaterials* 2014;35(8):2436–2445;
50. Zhang Y, Zhu D, Wei Y, et al. A collagen hydrogel loaded with HDAC7-derived peptide promotes the regeneration of infarcted myocardium with functional improvement in a rodent model. *Acta Biomater* 2019;86:223–234;
51. Shafiq M, Zhang Y, Zhu D, et al. In situ cardiac regeneration by using neuropeptide substance P and IGF-1C peptide eluting heart patches. *Regen Biomater* 2018;5(5):303–316;
52. Hassan S, Rezaei Z, Luna E, et al. Injectable self-oxygenating cardio-protective and tissue adhesive silk-based hydrogel for alleviating ischemia after MI Injury. *Small* 2024;20(32):e2312261;
53. Segers VF, Tokunou T, Higgins LJ, et al. Local delivery of protease-resistant stromal cell derived factor-1 for stem cell recruitment after myocardial infarction. *Circulation* 2007;116(15):1683–1692;
54. Ahmad Shiekh P, Anwar Mohammed S, Gupta S, et al. Oxygen releasing and antioxidant breathing cardiac patch delivering exosomes promotes heart repair after myocardial infarction. *Chem Eng J* 2022;428:132490;
55. Hong HS, Lee J, Lee E, et al. A new role of substance P as an injury-inducible messenger for mobilization of CD29⁺ stromal-like cells. *Nat Med* 2009;15(4):425–435;

56. Shafiq M, Kim SH. Biomaterials for host cell recruitment and stem cell fate modulation for tissue regeneration: Focus on neuropeptide substance P. *Macromol Res* 2016;24(11):951–960;
57. Hong HS, Kim S, Lee S, et al. Substance-P prevents cardiac ischemia-reperfusion injury by modulating stem cell mobilization and causing early suppression of injury-mediated inflammation. *Cell Physiol Biochem* 2019;52(1):40–56;
58. Kim JH, Jung Y, Kim BS, et al. Stem cell recruitment and angiogenesis of neuropeptide substance P coupled with self-assembling peptide nanofiber in a mouse hind limb ischemia model. *Biomaterials* 2013;34(6):1657–1668;
59. Wang K, Yao SY, Wang Z, et al. A Sequential dual functional supramolecular hydrogel with promoted drug release to scavenge ROS and stabilize HIF-1 α for myocardial infarction treatment. *Adv Healthc Mater* 2024;13(6):e2302940;
60. Yu C, Qiu Y, Yao F, et al. Chemically programmed hydrogels for spatiotemporal modulation of the cardiac pathological microenvironment. *Adv Mater* 2024;36(32):e2404264;
61. Garbern JC, Lee RT. Heart regeneration: 20 years of progress and renewed optimism. *Dev Cell* 2022;57(4):424–439;
62. Pomeroy JE, Helfer A, Bursac N. Biomaterializing the promise of cardiac tissue engineering. *Biotechnol Adv* 2020;42:107353;
63. Purcell BP, Lobb D, Charati MB, et al. Injectable and bioresponsive hydrogels for on-demand matrix metalloproteinase inhibition. *Nat Mater* 2014;13(6):653–661;
64. Zhao Y, Rafatian N, Feric NT, et al. A platform for generation of chamber-specific cardiac tissues and disease modeling. *Cell* 2019;176(4):913–927.e18;
65. Fiorino E, Rossin D, Vanni R, et al. Recent insights into endogenous mammalian cardiac regeneration post-myocardial infarction. *Int J Mol Sci* 2024;25(21):11747;
66. Yang H, Qin X, Wang H, et al. An in vivo miRNA delivery system for restoring infarcted myocardium. *ACS Nano* 2019;13(9):9880–9894;
67. Dushpanova A, Agostini S, Ciofini E, et al. Gene silencing of endothelial von Willebrand factor attenuates angiotensin II-induced endothelin-1 expression in porcine aortic endothelial cells. *Sci Rep* 2016;6:30048;
68. Bheri S, Davis ME. Nanoparticle–hydrogel system for post-myocardial infarction delivery of microRNA. *ACS Nano* 2019;13(9):9702–9706;
69. Marbán E. Deconstructing regenerative medicine: From mechanistic studies of cell therapy to novel bioinspired RNA drugs. *Circ Res* 2024;135(8):877–885;
70. Secco I, Giacca M. Regulation of endogenous cardiomyocyte proliferation: The known unknowns. *J Mol Cell Cardiol* 2023;179:80–89;

71. Burjanadze G, Gorgodze N, Aquaro GD, et al. Delayed miR-199a administration after myocardial infarction precludes pro-regenerative effects. *JACC Basic Transl Sci* 2025;10(5):634–649;
72. Menasche P, Renault NK, Hagège A, et al. First-in-man use of a cardiovascular cell-derived secretome in heart failure. Case report. *EBioMedicine* 2024;103:105145;